MICROSTRUCTURAL FEATURES OF A NEW MARTENSITIC STEEL HEAT TREATMENT: QUENCHING AND PARTITIONING

David V. Edmonds and Kejian He – Institute for Materials Research, University of Leeds, Leeds, LS2 9JT, United Kingdom
Fernando C. Rizzo – Department of Materials Science and Metallurgy, Pontificia Universidad Catolica-Rio de Janeiro, RJ 22453-900, Brazil
Amy Clarke, David K. Matlock and John G. Speer - Advanced Steel Processing and Products Research Centre, Colorado School of Mines, Golden, CO 80401, USA

ABSTRACT

A new idea for the heat treatment of martensite, different to customary quenching and tempering, is first explained: the new process involves quenching to a temperature between the martensite-start (M_s) and martensite-finish (M_f) temperatures, followed by ageing, either at, or above, the initial quench temperature, whereupon carbon can partition from the supersaturated martensite phase to the untransformed austenite phase, thereby increasing its stability upon subsequent cooling to room temperature. This new treatment has been termed 'Quenching and Partitioning' (Q&P), to differentiate it from quenching and tempering (Q&T), and could be used to create microstructures with martensite/austenite combinations with potentially attractive properties. However, to be effective, it is necessary to protect the carbon from competing reactions during the partitioning treatment, principally carbide precipitation, and this aspect has been examined in the present work. Firstly, the volume fraction and morphology of the untransformed austenite will depend upon the quench temperature. This will influence the partitioning behaviour, including the kinetics and perhaps the final solute carbon concentration of the austenite, along with the sequence of possible competing reactions, which are themselves also affected by the choice of partitioning temperature. Si additions can be used successfully to suppress cementite formation, but this element has less effect upon the formation of transitional carbides such as epsilon carbide. Combinations of quench and partitioning temperatures, allied to the alloying approach and kinetics of partitioning, must be chosen in order to locate the heat treatment window that will maximize the extent of carbon partitioning and hence control the stabilisation of the austenite, to achieve the optimum structure and properties. Some aspects of the mechanical behaviour of a quenched and partitioned TRIP steel recently examined are presented.

KEYWORDS

Steel heat treatment; Martensite; Retained austenite; Carbon partitioning; Carbide precipitation; Diffusion kinetics; Bainite transformation; Bar steel; TRIP steel; Mechanical behaviour.

INTRODUCTION

Quenching and tempering heat treatments have long been successfully applied to steels to produce good combinations of strength and toughness from martensitic microstructures [eg 1]. During tempering the carbon supersaturation in the martensite is reduced by carbide precipitation, lowering hardness and strength, but relieving internal stress and improving toughness. Any residual untransformed austenite is also decomposed, improving microstructural stability. The present paper

HOME

reports on the development of a novel way to develop a new form of microstructure [2-10], based also upon quenched martensite, but by deploying a heat treatment sequence that achieves almost the opposite: *suppression of carbide precipitation* and *stabilisation of residual austenite*. Instead of relieving carbon supersaturation in the martensite by carbide precipitation, the latter is suppressed by suitable alloying, giving sufficient time for carbon to escape from the martensitic laths or plates to the untransformed austenite, raising its carbon level and achieving its retention. Thus, residual austenite is first encouraged by only a partial quench, to a temperature between the martensite-start (M_s) and martensite-finish (M_f) temperatures, followed by a 'partitioning' treatment either at, or above, the initial quench temperature, designed to enrich the remaining untransformed austenite with carbon escaping from the supersaturated martensite phase. This form of heat treatment produces a microstructure that comprises an aggregate of ferrite (martensite) and carbon-enriched stabilised austenite, similar to so-called 'carbide-free bainite' microstructures [11-13], of recent interest with respect to high-strength steels [14-18], including more recently, 'hard bainite' [eg 19,20], to automotive TRIP steels [eg 21,22] and to austempered ductile irons [eg 23-28]. This procedure, illustrated by Fig. 1 [3, 4], has been termed 'Quenching and Partitioning' (Q&P), to distinguish it from quenching and tempering. The emphasis of the work presented in this paper is to explore and confirm the sequence of microstructural changes that occur during evolution of the microstructure by this heat treatment procedure.

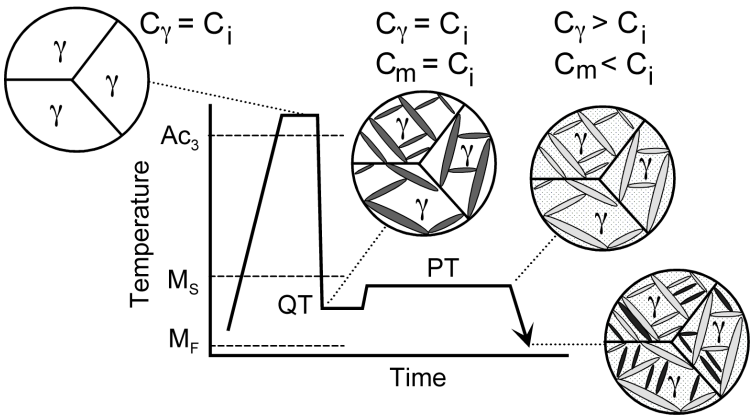

Fig. 1 Schematic Q&P heat treatment process producing austenite/martensite microstructures, as appropriate, from homogeneous austenite [20,21]. (C_i, C_γ, and C_m represent the carbon contents of the initial alloy, austenite, and martensite, respectively, and QT and PT are the quenching and partitioning temperatures, respectively.)

BACKGROUND TO THE Q&P HEAT TREATMENT CONCEPT

Thermodynamics of Carbon Partitioning

Austenite decomposition at sub-critical low temperatures, where long-range diffusion of carbon can occur but partitioning of slow-moving substitutional elements is difficult, is described by paraequilibrium [29-31]. Under this condition, where the interface is normally mobile, requiring short-range movements of iron and substitutional atoms, the ferrite/austenite phase fractions can adjust to

ensure that the requirement for equal chemical potentials (or partial molar free energies) of each component (Fe, substitutionals and C) in both ferrite and austenite is met. However, under the conditions imposed by the Q&P heat treatment, the austenite/ferrite phase fractions are fixed by the initial quench. Thus, during the subsequent partitioning treatment, the interface between martensite and untransformed austenite is assumed to be *stationary*, precluding even short-range diffusion of iron and substitutionals. In this case of an immobile or constrained interface between the two phases, the metastable ferrite/austenite equilibrium reached by the completion of carbon partitioning has thus been termed *"constrained carbon equilibrium"* or CCE [2,6,32-34].

This situation is described by two conditions: equal chemical potential of carbon in each phase, and conservation of iron (and substitutional) atoms in each phase. The CCE states for two arbitrary examples, where the tangents to the ferrite and austenite free energy curves intersect the carbon axis at a single point, indicating equal carbon potentials in ferrite and austenite, but where the chemical potential of iron is clearly different in each phase, are illustrated in Fig. 2(a), alongside the normal metastable equilibrium (Fig. 2(b)). Consequently, an infinite set of possible ferrite and austenite phase compositions exists, with the applicable one uniquely determined by the conservation condition of the matter balance.

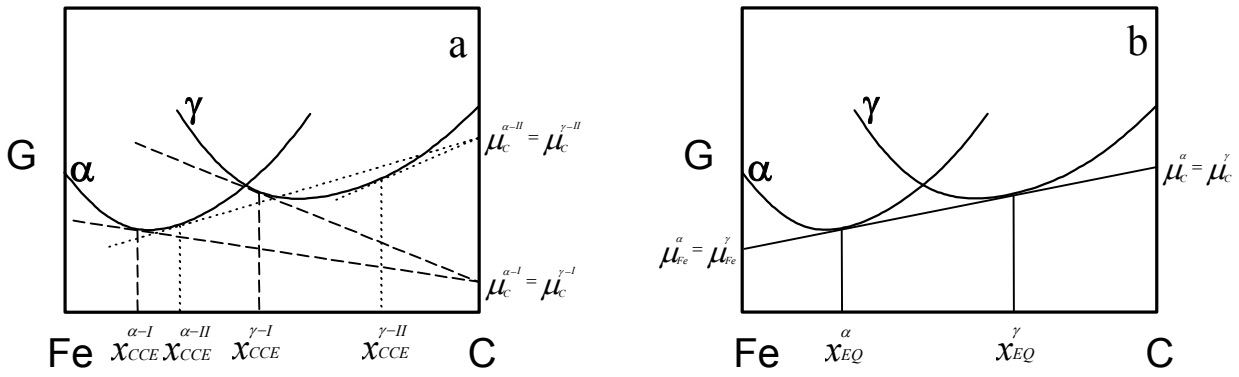

Fig. 2 Schematic molar Gibbs free energy versus composition diagrams illustrating metastable equilibrium at a particular temperature between ferrite and austenite in the Fe-C binary system: (a) constrained carbon equilibrium conditions (I and II) showing two possible ferrite and austenite compositions satisfying the CCE requirement that the chemical potential of carbon is equal in the two phases, and (b) normal equilibrium [2].

Thus it is demonstrated that for CCE the phase fractions are determined by the extent of the martensite reaction at the quench temperature and not by the lever rule applied using an equilibrium or paraequilibrium tie-line. The extent of carbon partitioning may then be calculated by combining the thermodynamic requirement with the mass balance requirement according to the total carbon concentration and volume fractions of martensite and untransformed austenite determined by the quench temperature (obtainable from the Koistinen and Marburger relationship) [2,35]. This shows that most of the carbon in the steel is expected to partition to the austenite, to give high levels of carbon enrichment (eg Fig. 3), and hence strong potential for austenite stabilisation.

HOME

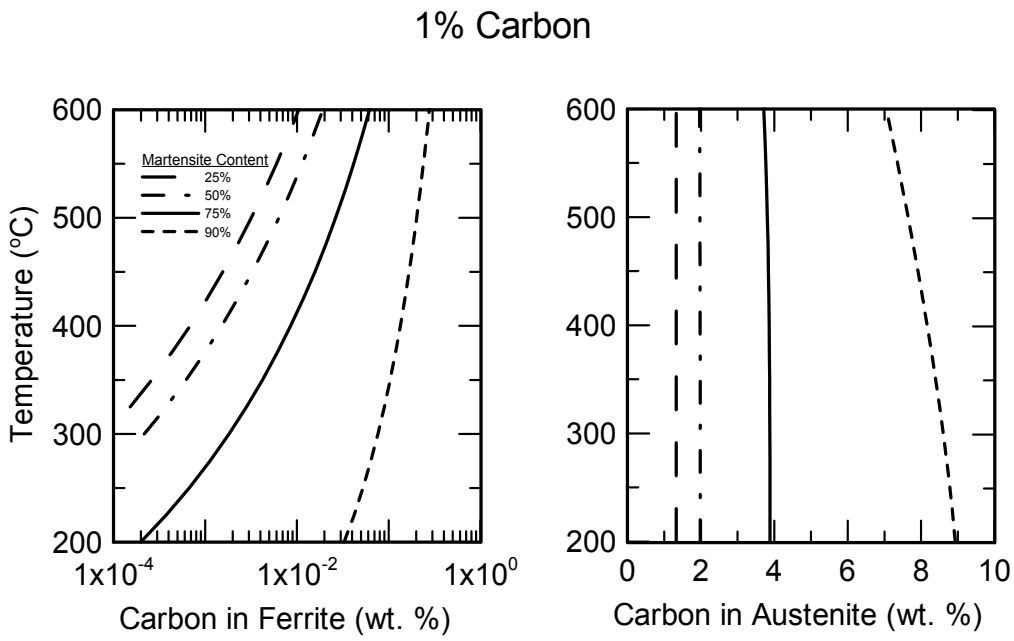

Fig. 3 Carbon concentrations in ferrite and austenite for the CCE condition, as a function of partitioning temperature, for different martensite and austenite volume fractions, calculated for Fe-1.0 C (wt%) [2].

Heat Treatment Design

The schematic diagram showing the heat treatment cycle, presented in Fig. 1 [3,4], also summarises the hypothesized sequence of microstructures evolving from homogeneous austenite during Q&P processing. As the untransformed austenite is enriched with carbon during partitioning, its effective M_s - M_f temperature range is suppressed. For complete chemical stabilisation of austenite the M_s must be depressed to room temperature or below, otherwise some additional 'fresh' as-quenched martensite will be present at room temperature. The microstructural sequence during the processing of TRIP sheet steel essentially differs only by the presence of intercritical ferrite from solution treatment carried out in the two-phase region In this case the overall carbon concentration of the steel will be concentrated into the smaller volume fraction of austenite before quenching, and the potential for stabilising the austenite is therefore influenced (lower M_s) in comparison with heat-treating of homogeneous austenite.

The efficient stabilisation of austenite is consequently a balance between the fraction of austenite, determined by the quench temperature, and the *available* carbon. If competing reactions are ignored, the latter is determined by the carbon concentration of the steel and also by the quench temperature, which gives the fraction of martensite, which is the *source* of *additional* carbon during the partitioning treatment. Two extremes can be considered: at a high quench temperature (just beneath M_s) only a small fraction of martensite is formed, and so the large balance of untransformed austenite inherits only a small amount of additional carbon during partitioning, resulting in little extra chemical stabilisation, whereas, at a low quench temperature (just above M_f), a large volume of martensite is formed, discarding its carbon into a correspondingly small fraction of untransformed austenite – the chemical stability of this austenite is assured at room temperature, but its volume fraction, determined by the low quench temperature, remains low. If the maximum austenite fraction is desired, it is necessary to

HOME

identify the quench temperature between these extremes that produces just the right amount of martensite required to enrich the untransformed austenite with carbon, after full partitioning, to reduce its M_s temperature to room temperature.

A simple method for determining this optimum quench temperature has been developed [3], assuming that competing reactions are avoided and that all of the carbon partitions from martensite to austenite. The relative fractions of martensite and untransformed austenite at the quench temperature are calculated from the undercooling below M_s, based upon the Koistinen-Marburger relationship, with the M_s for the applicable austenite carbon content estimated from published correlations. (In the case of intercritically-annealed TRIP steels, it can be assumed that all of the carbon is in the austenite prior to quenching, as the solubility of carbon in ferrite is very low.) Then, by applying the Koistinen-Marburger relationship again, this time to the carbon-enriched untransformed austenite fraction after full partitioning, the final phase fractions after final cooling can be predicted.

Figure 4 illustrates the predictions according to this methodology [3,36], for both homogeneous austenite and intercritically-annealed austenite in two different steel compositions, indicating the optimum quench temperatures for yielding the maximum amount of retained austenite.

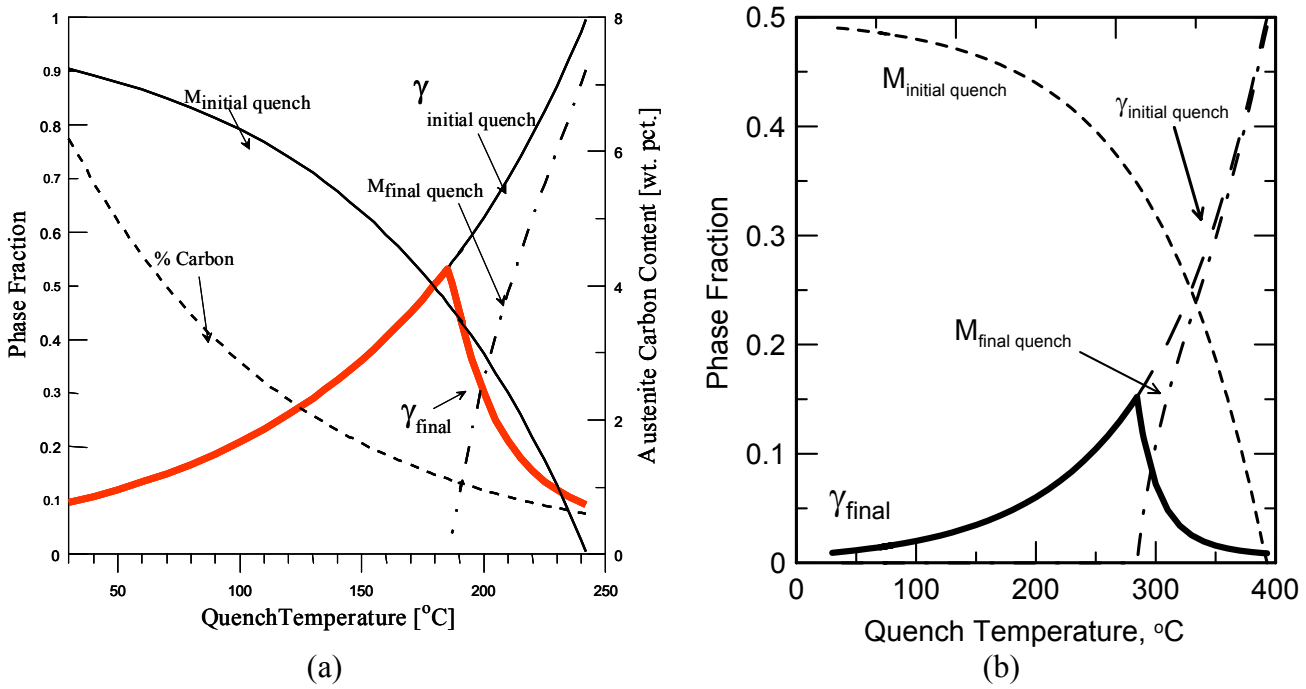

Fig. 4 Predicted components of the microstructure after Q&P treatment for (a) an experimental 0.6wt%C bar steel [36], and (b) a high-Al TRIP sheet steel containing 50% intercritical ferrite [3]. (The solid bold line gives the final austenite fraction at room temperature, whilst the dashed lines represent the austenite (γ) and martensite (M) present at the initial quench temperature, and the additional 'fresh' martensite formed during the final quench to room temperature.)

HOME

Kinetics of Carbon Partitioning

A critical step in the Q&P process is the escape of carbon from the martensite laths or plates to the untransformed austenite during the partitioning treatment. It is critical because it competes with the formation of carbides in the martensite, the normal characteristic of the tempering process. Once in the austenite, the risk of carbide formation is considered to be much reduced, for instance, it is reported [37] that carbide precipitation from untransformed interlath austenite observed in the lower bainite reaction is much slower than the dominant carbide precipitation that occurs within the bainitic ferrite. The carbon also needs to homogenise within the austenite in order to protect it fully against any decomposition to 'fresh' martensite upon cooling to room temperature.

The partitioning of carbon from martensite to austenite has been simulated [8] using DICTRA software [38], with the assumption that only carbon equilibrates its chemical potential at the interface [39]. Two side-by-side plate-shaped regions of martensite and austenite were assumed, of average thickness 0.3 and 0.14 μm, respectively, based upon transmission electron microscopy measurements. Figure 5 shows the evolution of the carbon concentration profile in the martensite and austenite regions, for times ranging from 0.0001 to 10 seconds, for a steel with composition 0.19%C-1.59%Mn-1.63%Si partitioned at 400ºC.

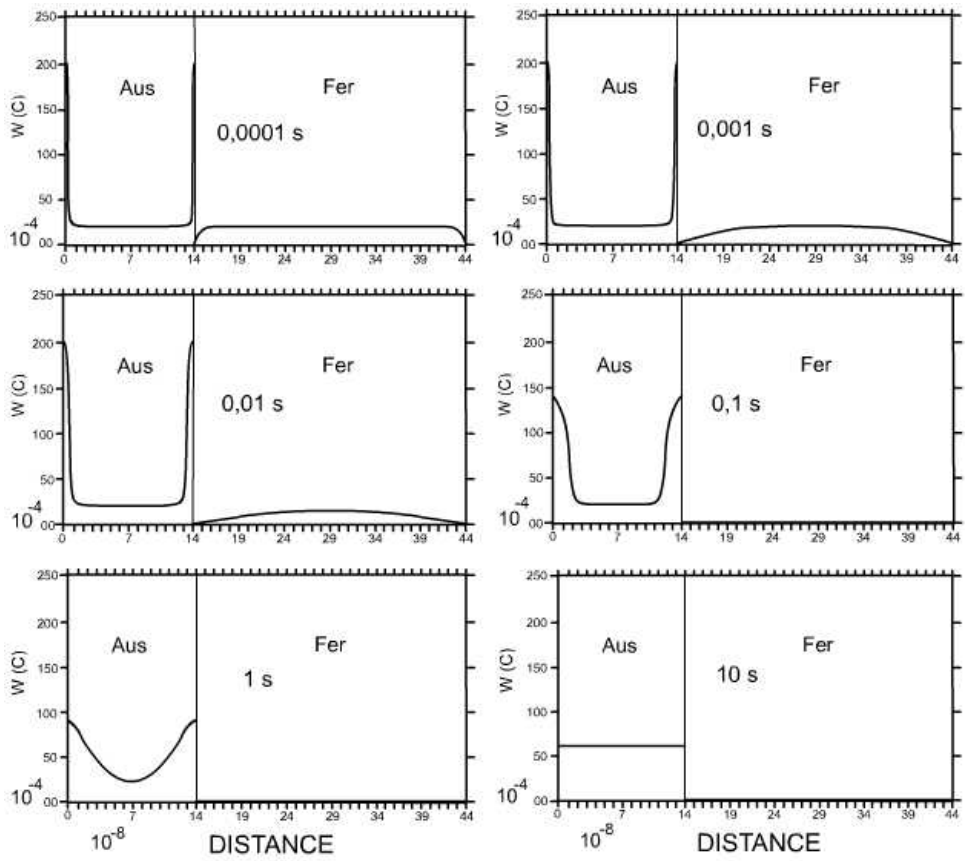

Fig. 5 Carbon concentration profiles (wt %) in the ferrite and adjacent austenite during partitioning at 400˚C for times ranging from 10^{-4} to 10 seconds, calculated for Fe-0.19%C-1.59%Mn-1.63%Si [8].

HOME

It is revealed, for the conditions considered, that the martensite is depleted of its carbon in less than 0.1 seconds, but that it takes around 10 seconds to homogenise the austenite (which is also roughly half the width of the martensite in this example). The calculations indicate that the mobile carbon is likely to have escaped from the martensite in times well within those customarily used for industrial heat treatments. However, the calculations have relevance to the likely chances for inhibition of competing carbide precipitation within the ferrite [8]. Although Fig. 5 indicates that a martensite plate should be depleted of its carbon in around 0.1 seconds, the driving force for carbide precipitation starts decreasing much earlier, as soon as the carbon concentration begins to fall. The time period available for carbide precipitation in the martensite may thus be estimated from the time before impingement of the diffusion fields at the centre of the plate, represented by the moment at which the carbon flux reaches the centre of the plate. Figure 6(a) shows how the carbon concentration in the centre of the martensite (ferrite) plate varies with time during partitioning, whilst Fig. 6(b) shows the flux of carbon. It is reasonable to estimate the period available for carbide precipitation, before the carbon flux is substantial in the centre of the plate, at about 10^{-3} seconds.

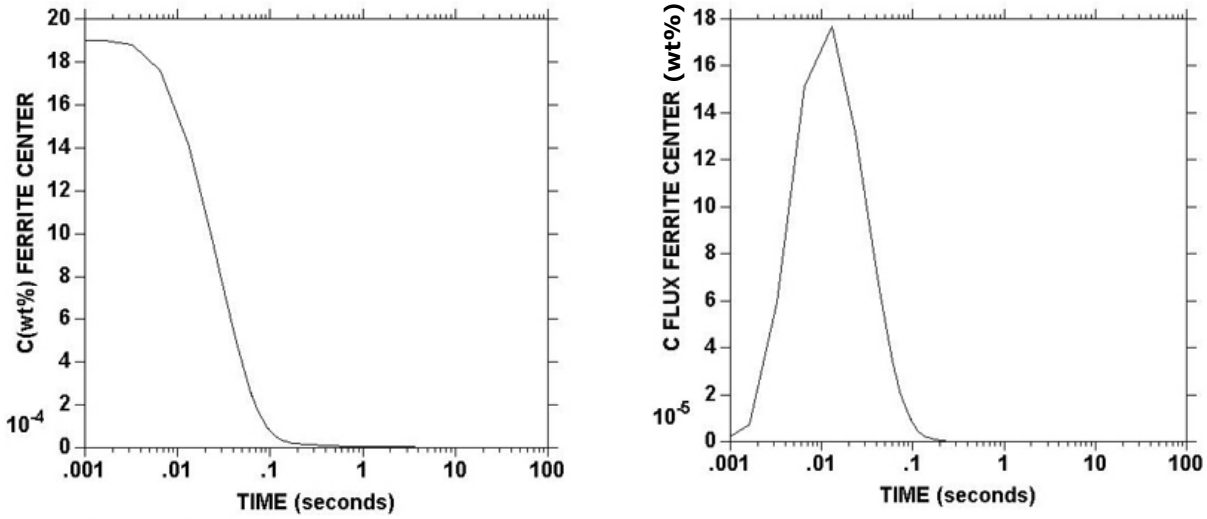

(a) (b)

Fig. 6 (a) Carbon concentration and (b) carbon flux in the centre of a ferrite plate-shaped region, as a function of time.

The calculations show that homogenisation of the austenite is some two orders of magnitude slower than carbon depletion of the martensite. Consequently, even though carbon depletion of the martensite plate, and hence the corresponding enrichment of the adjacent austenite plate, is virtually complete after 0.1 seconds (Fig. 5), at this point most of the carbon remains concentrated in a thin region of austenite adjacent to the interface, and the majority of the austenite plate still has its original carbon composition. Thus it can be hypothesised that the stabilisation of the austenite occurs progressively, from the interfaces towards the centres of the austenite regions, following the inward advance of the increased carbon concentration corresponding to an M_s at room temperature [9]. Therefore, by applying the Koistinen-Marburger relationship at each point across the austenite plate-shape the carbon concentration profile (Fig. 7(a)) can be exchanged for a profile of stabilised austenite (Fig. 7(b)) [9]. The final theoretical austenite phase fraction, as a function of quench temperature, can then be re-calculated (Fig. 8), taking into account these kinetics for migration of the carbon across the austenite region, whereupon it has been found that beneath the optimum quench temperature (for QT=180ºC)

HOME

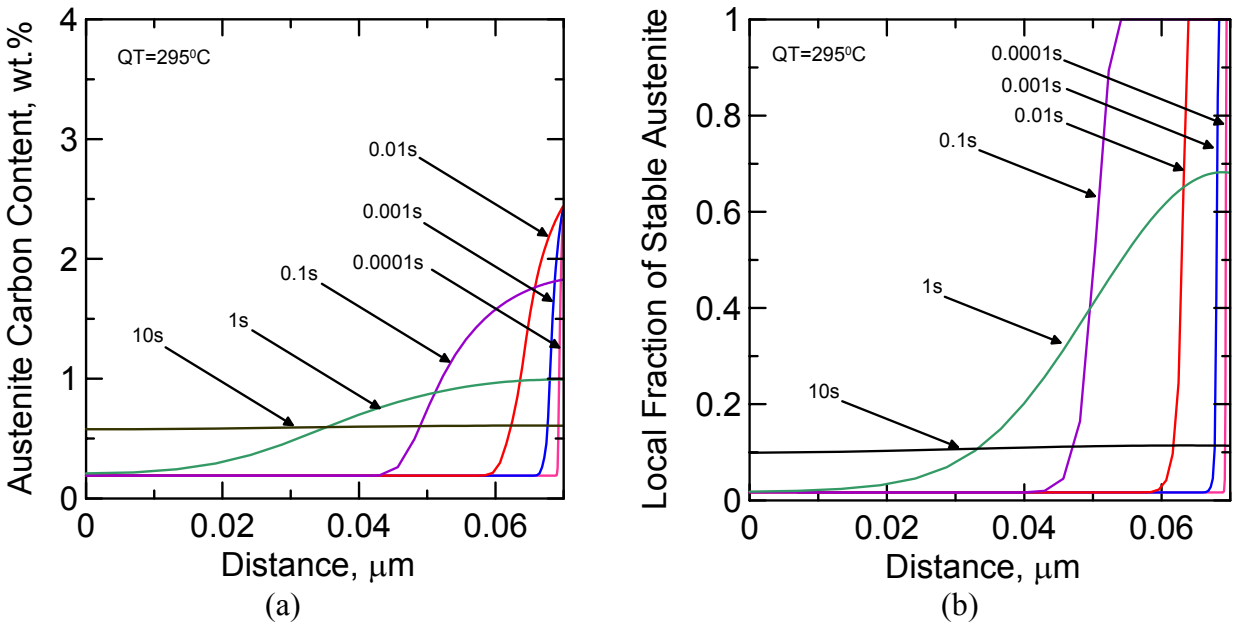

Fig. 7 Schematic diagrams of (a) the carbon concentration profile across an austenite plate-shaped region, and (b) the corresponding fraction of stabilised austenite [9], calculated for times in the range 10^{-4} to 10 seconds, for Fe-0.19%C-1.59%Mn-1.63%Si partitioned at 400ºC. (Both figures represent a half-plate with centre on the left and interface on the right.)

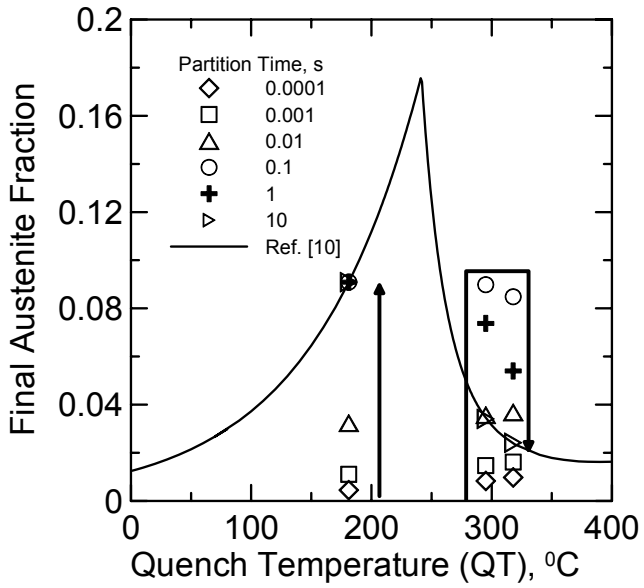

Fig. 8 Final austenite fraction versus quench temperature after full austenitisation for a 0.19%C-1.59%Mn-1.63%Si composition. The solid curve is constructed without taking into account the calculated partitioning kinetics [9], whereas individual data points incorporate the partitioning kinetics. (Ref [10] in this figure refers to Ref [3] in the present paper.)

HOME

maximum stabilisation is achieved after 0.1s, but that above the optimum quench temperature (for QT=295ºC and 320ºC), the theoretical maximum can be *exceeded* for intermediate times, 0.1s roughly doubling the stable austenite fraction, from 4 to 9%, before it settles at the theoretical level after 10s. This indicates that the kinetics of partitioning may well affect the potential to stabilise austenite, of possible practical importance to industrial processes, particularly in potentially widening the range of quench temperatures delivering substantial fractions of stabilised austenite. It should be noted that the points plotted in Fig. 8 were specifically calculated to incorporate the kinetics of partitioning at 400°C, and that partitioning at different temperatures would affect the associated kinetics.

EVOLUTION OF THE Q&P MICROSTRUCTURE

Examples of the composition ranges of a number of experimental and commercial steels that have so far been examined are given in Table 1. These have been mainly representative of medium carbon bar steels and lower carbon sheet steels, with enhanced Si or Al additions. The Q&P heat treatments mainly comprised: for medium carbon levels - austenitising at 900ºC for 300 s followed by quenching to the range 150-210ºC and partitioning in the range 250-500ºC for 10-3600 s; for low carbon levels - annealing at either 950ºC, 900°C or 820ºC for 180 s (to achieve either full austenitisation or intercritical ferrite, respectively) followed by quenching to the range 200ºC - 260ºC (holding for 3-10 s) and partitioning in the range 350ºC - 450°C for 10-1000 s. Salt baths were used for austenitising, intercritical annealing, and partitioning treatments, and a tin-bismuth or a low temperature molten salt bath was used for the lower quenching temperature treatments. Final quenching was into water. Experimental details regarding the heat-treatment of the high-Al sheet steel composition are published elsewhere [3].

Table 1 Concentration (wt%) of principal elements in experimental steels.

	C	Mn	Si	Al
Bar	0.60	0.95	1.96	-
	0.35	1.30	0.74	-
Sheet	0.19	1.59	1.63	-
	0.19	1.46	0.02	1.96

Quenching Treatment

It is difficult with the Q&P heat treatment sequence to examine the starting microstructure before partitioning, because this is created and exists only at the quench temperature between M_s and M_f, characteristically well above room temperature for the carbon and low alloy steels of current interest. However, inferences can be drawn from an interrupted quench to room temperature. Figure 9 shows typical examples of light and electron micrographs of quenched martensite structure in one of the experimental steels (Fe-0.60%C-0.95%Mn-1.96%Si) quenched first to a temperature between M_s and M_f, equilibrated for 120 s, and then given a final quench to room temperature. Examination by X-ray diffraction revealed >6% retained austenite after interrupted quenching as compared with <2% after direct quenching [36], illuminated in dark-field using an austenite reflection in Fig. 9(c). This suggests carbon enrichment of austenite at the initial quench temperature, the additional carbon partitioning from a martensite fraction that must therefore have been present. Additionally, there is some evidence

of carbide precipitation, thought but not proven unambiguously to be transitional epsilon carbide, in the martensite after interrupted quenching, indicated by the arrow in the bright-field TEM micrograph of Fig. 9(b). Both observations are plausible confirmation that a mixed martensite/untransformed austenite structure was present at the initial quench temperature between M_s and M_f, as required.

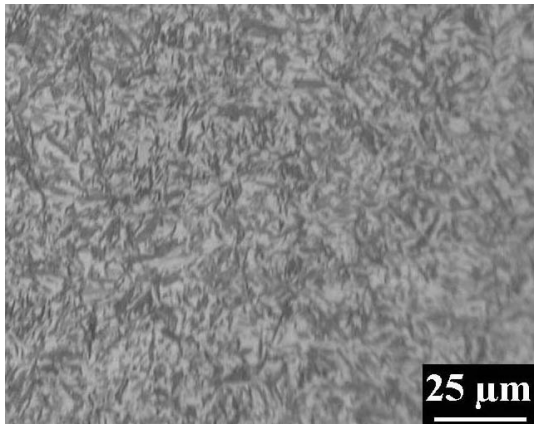

(a)

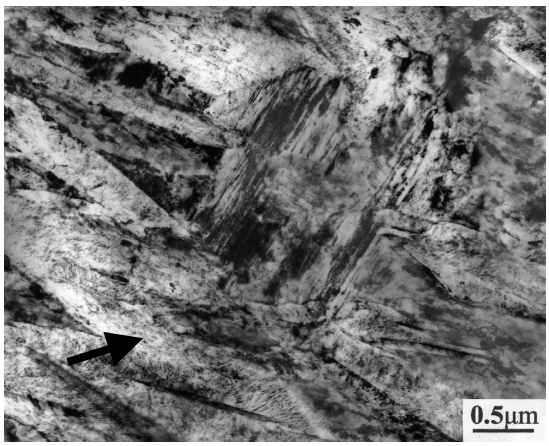

(b)

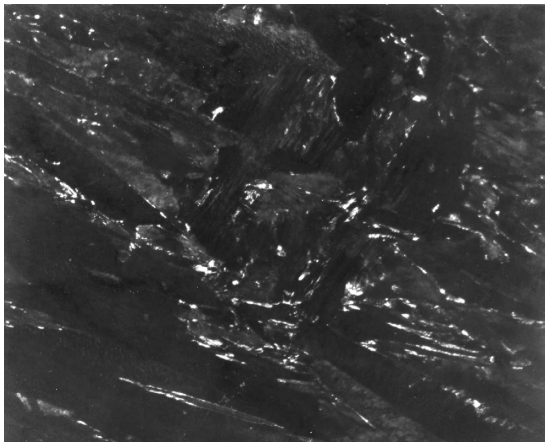

(c)

Fig. 9 Microstructures of grade 9260 bar steel (Fe-0.60%C-0.95%Mn-1.96%Si) quenched to 190ºC, held for 120 s, and then quenched to room temperature: (a) light micrograph, (b) TEM bright-field image and (c) TEM dark-field image using the (002) austenite reflection [5].

Partitioning Treatment

Partitioning treatments above the initial quench temperature, and above the Ms, fall into the bainite transformation temperature range. It is thus instructive to determine the microstructural differences between steel subjected to the Q&P treatment, or to an austempering treatment at the same (partitioning) temperature to produce bainite. Figure 10 compares micrographs obtained by both light and electron microscopy, of the two heat treatment routes in medium carbon grade 9260 steel (Fe-0.60%C-0.95%Mn-1.96%Si) for treatment at 400°C. The Q&P microstructure appears significantly different than the austempered microstructure: the former has the characteristics of a martensitic

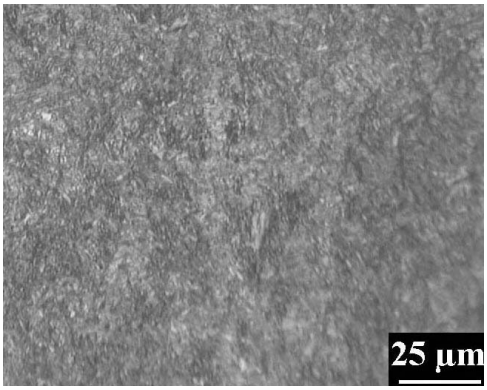

(a)

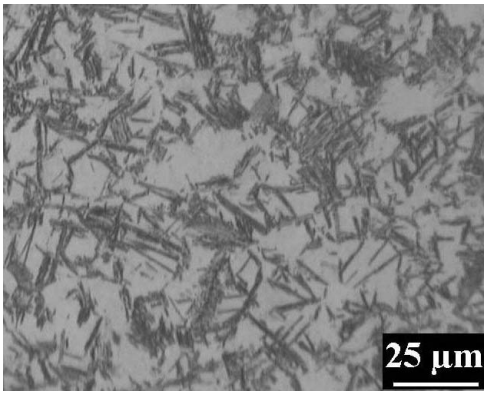

(d)

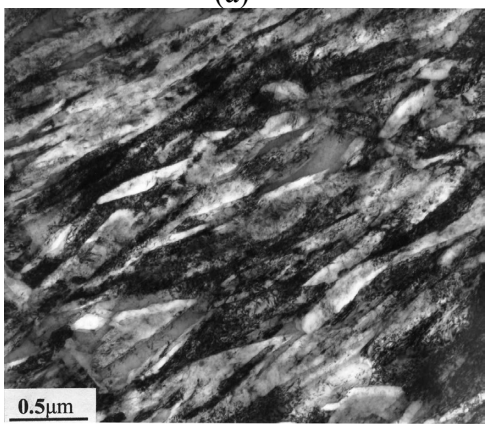

(b)

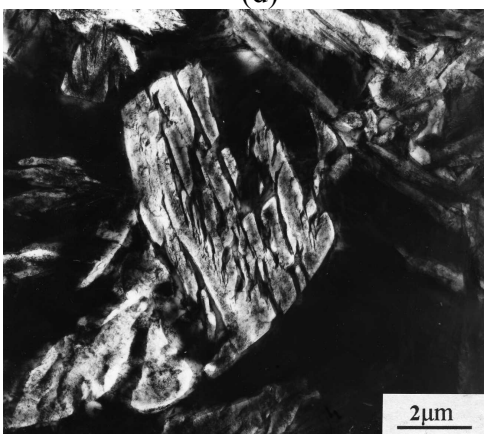

(e)

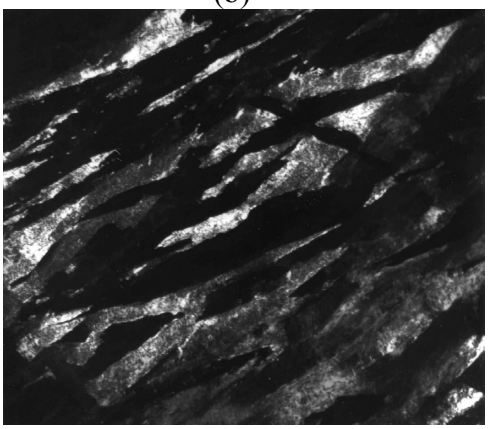

(c)

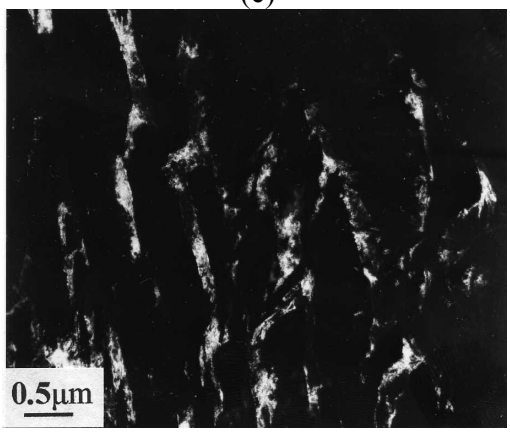

(f)

Fig. 10 Microstructures of grade 9260 bar steel (Fe-0.60%C-0.95%Mn-1.96%Si) given either a Q&P treatment with partitioning at 400ºC for 120 s (for QT=190ºC) (a-c), or an austempering treatment at 400ºC for 120 s (d-f): (a) light micrograph, (b) TEM bright-field image and (c) TEM dark-field image using the (002) austenite reflection, of Q&P structure [10]; (d) light micrograph, (e) TEM bright-field image and (f) TEM dark-field image (of central region of (e)) using the (420) austenite reflection, of austempered structure.

HOME

structure, eg highly dislocated laths in a packet arrangement, with films of retained austenite detectable between the laths/plates, whilst the latter has the generally courser, more feathery appearance associated with bainite, but with austenite films interwoven with the bainitic ferrite plates, a characteristic of the 'carbide-free bainite' expected in a steel containing a high concentration of Si that will suppress bainitic carbide formation [11-13]. The observations recorded in Fig. 10 are the result of specific comparative experiments on a fully austenitised medium carbon steel, but the two microstructures can be similarly distinguished in lower carbon TRIP steels compared either after conventional heat treatment to give bainitic regions, or after a Q&P treatment. Two important conclusions may be drawn from these observations; firstly, that Q&P produces a different microstructure (and generally more refined microstructure) than austempered bainite, and that also, the two forms of microstructure may be differentiated. This is important because the bainite transformation can be a 'competing reaction' that could reduce the maximum volume of retained austenite attainable.

Figure 11 illustrates the Q&P structure in the medium carbon grade 9260 steel (Fe-0.60%C-0.95%Mn-1.96%Si) after partitioning for 900 s at 500°C. After such longer times, especially in the higher temperature range, less austenite can be stabilised and retained owing to competition with other possible alternative reactions. In this case no retained austenite films were detected, but a distribution of coarse cementite is visible, both within the ferrite plates (indicative of competition with carbon escape from the martensite) and at plate boundaries (indicative of precipitation in the austenite or most probably at the austenite/martensite interfaces).

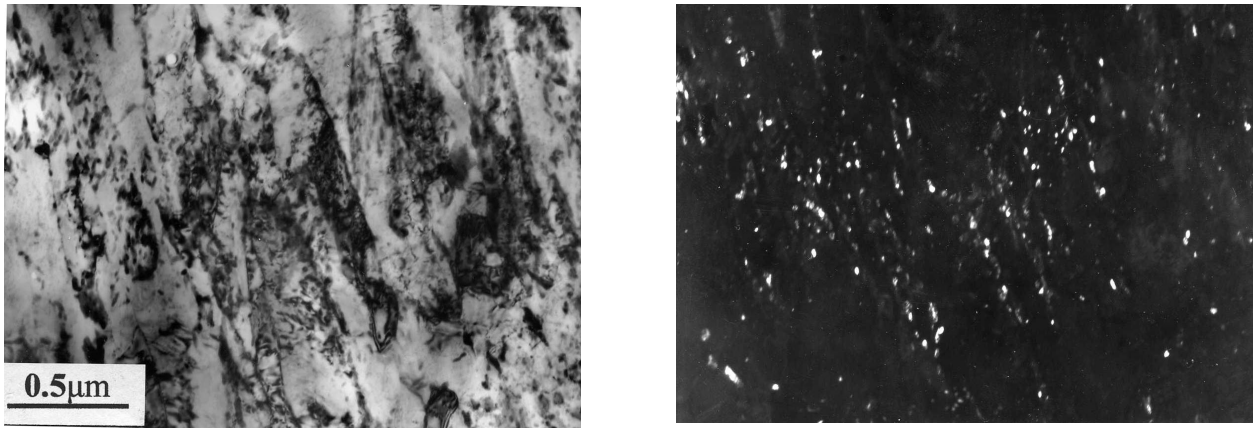

(a) (b)

Fig. 11 Q&P microstructure in a medium carbon grade 9260 bar steel (Fe-0.60%C-0.95%Mn-1.96%Si) after quenching to 190°C and partitioning for 900 s at 500°C: (a) TEM bright-field image, and (b) TEM dark-field image using the (202) cementite reflection.

As mentioned already, the partitioning treatment can be at, or above, the initial quench temperature. The results described above in respect of the observations shown in Fig. 9 confirm that both partitioning of carbon from martensite to untransformed austenite, and a carbide precipitation reaction competing for carbon in the martensite, have already begun at the initial quench temperature in this example.

HOME

Figure 12 shows the experimental variation in retained austenite fraction, measured by X-ray diffraction, after Q&P treatment in bar steel grade 9260 (Fe-0.60%C-0.95%Mn-1.96%Si) as compared with the maximum austenite achievable according to the theory described above (Fig. 4) [36]. It can be seen that the experimental austenite phase fraction follows the predicted relationship with quench temperature for this partitioning treatment, but at a reduced level. This indicates the probable intervention of competing reactions that have either lowered the concentration of additional escaping carbon available to the untransformed austenite during the partitioning treatment, or reduced the

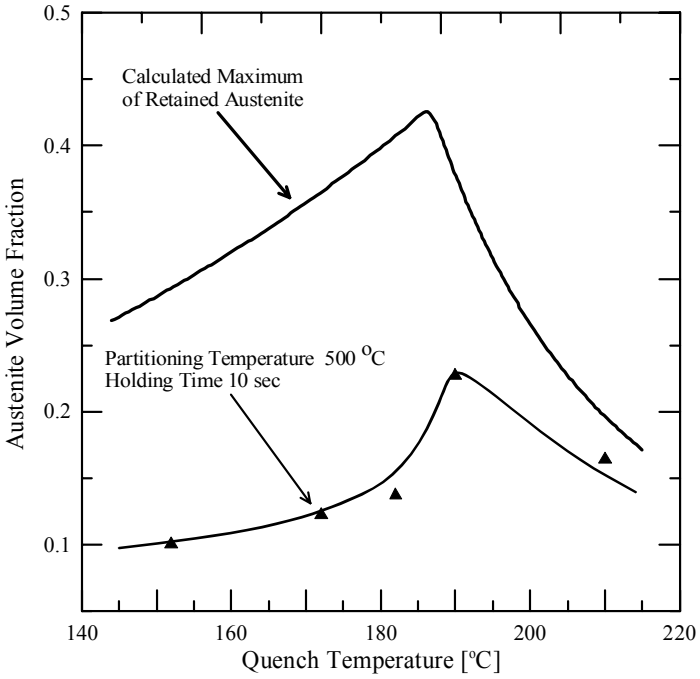

Fig. 12 Final volume fraction of retained austenite as a function of quench temperature, measured after a partitioning treatment of 10 s at 500ºC, and the calculated maximum fraction if full carbon partitioning is achieved over this quench temperature range for grade 9260 bar steel (Fe-0.60%C-0.95%Mn-1.96%Si) [36].

volume of untransformed austenite by its decomposition. These can include: amongst the first type of competing reaction; carbon trapping in the martensite; carbide precipitation in the martensite; carbide precipitation in the austenite; and amongst the second type; bainite transformation of the austenite; pearlite transformation of the austenite. The last of these is dependent upon intersection with the lowest portion of the diffusional transformation C-curve at the relatively low temperatures of interest, and thus is expected to initiate only after very long times, thought to be of marginal concern to industrial processes, and most likely to be preceded by the other alternative reactions. Less marginal might be decomposition of the residual austenite to bainite, most likely when large pools of untransformed austenite remain after the initial quench but which could be possible within the timescale of industrial processing, although less than required for escape of the carbon from the martensite phase. However, although expected to limit the amount of stabilised austenite achievable by the Q&P process, this bainite would be 'carbide-free' and also consist of a mixture of bainitic ferrite with retained austenite [11-13]. Thus, in the context of microstructural observations considered here, significance is attached to the potential individual carbide reactions, and for the reason already mentioned above, that carbide

HOME

precipitation within the austenite is expected to be sluggish compared with that in martensitic ferrite, attention is focused upon carbide precipitation within the martensite.

Figure 13(a) shows thin films of retained austenite between martensite laths after partitioning at 250ºC, and can be compared with Fig. 10(a) showing the thicker retained austenite films observed after partitioning at a higher temperature of 400ºC. Reduced austenite retention at the lower partitioning temperatures was found to be due to carbide precipitation in the martensite phase. Figure 13(b) shows copious precipitation, identified by electron diffraction (Fig. 13(c)) as transitional epsilon carbide, typical of that observed over the lower range of partitioning temperatures. Consequently, the alloying elements used to inhibit carbide reactions were ineffective in suppressing the occurrence of this phase sufficiently to allow escape of all of the carbon from the martensite. The dominant carbide at higher partitioning temperatures was cementite, for which the alloying did appear to be effective in suppressing its precipitation, such that for shorter times at the partitioning temperature very little cementite was detected, thereby giving ample time for enrichment of the untransformed austenite with carbon diffused from the adjacent martensite.

Silicon, and to a lesser extent, aluminium, are known to influence the sequence of reactions customarily observed during the tempering of martensitic steels [eg 40-42] or the course of the bainite reaction [eg 11-13,43,44], by retarding the formation of cementite and thus, either delaying the progress of Stage 3 tempering (principally, the formation of cementite at the expense of transitional epsilon carbide) or producing ‘carbide-free’ bainite. This suppression of cementite was first explained by the low solubility of Si in cementite, and thus a need to diffuse away from the growing carbide [40], and there has been more recent confirmatory experimental evidence that Si is rejected into the surrounding ferrite [45]. In contrast, Si appears to stabilise the transitional epsilon carbide during tempering, which consequently persists for longer times and to higher temperatures, and although this was thought to be due to higher silicon solubility in the transitional carbide [41], measurements by atom-probe and field emission STEM techniques have not indicated a particularly high level of enrichment [45]. The appearance of the transitional epsilon carbide therefore effectively defines the lowest practical partitioning temperature likely to achieve close to the theoretical maximum of austenite stabilisation.

For steel subjected to intercritical annealing, the behaviours described above are essentially the same, the only difference being the presence of intercritical ferrite in the final microstructure. The austenite phase, of course, will contain excess carbon, inherited from the intercritical ferrite region during intercritical annealing. Figure 14 shows thick austenite regions associated with partitioned martensite, similar to those mentioned above for medium carbon steels quenched from homogeneous austenite, in an intercritically annealed steel subjected to a Q&P treatment [9]. Intercritical ferrite is also visible in this micrograph.

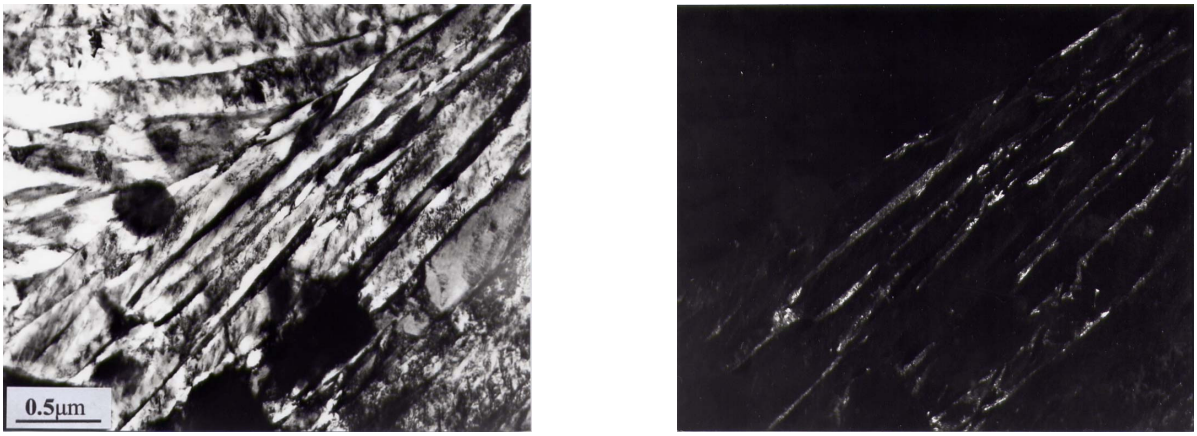

(a)

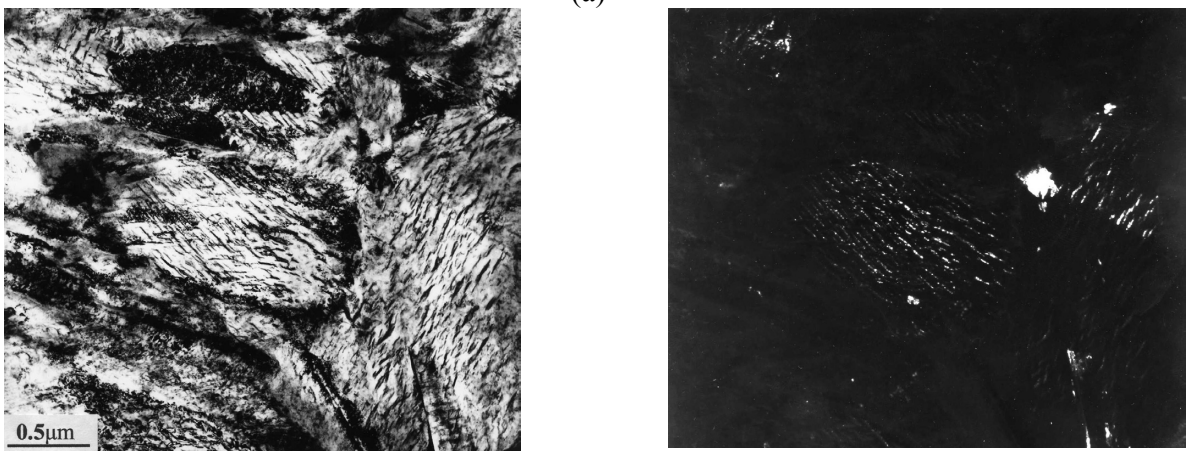

(b)

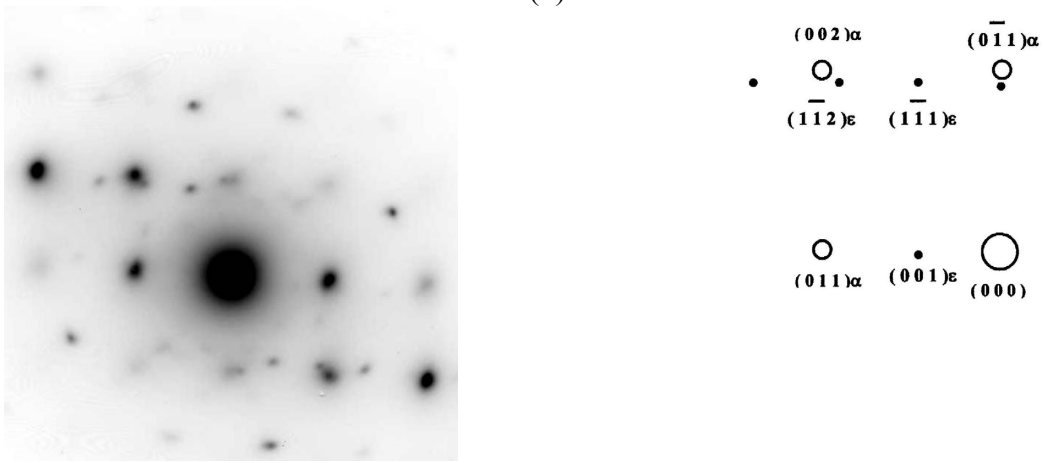

(c)

Fig. 13 Microstructures of grade 9260 bar steel (Fe-0.60%C-0.95%Mn-1.96%Si): (a) quenched to 190ºC and partitioned at 250ºC (bright field and dark field using (002) austenite reflection), (b) quenched to 150ºC and partitioned at 250ºC (bright field and dark field using (1-11) epsilon carbide reflection) [10], and (c) same area diffraction pattern from central region of (b) with schematic indexing identifying epsilon carbide.

HOME

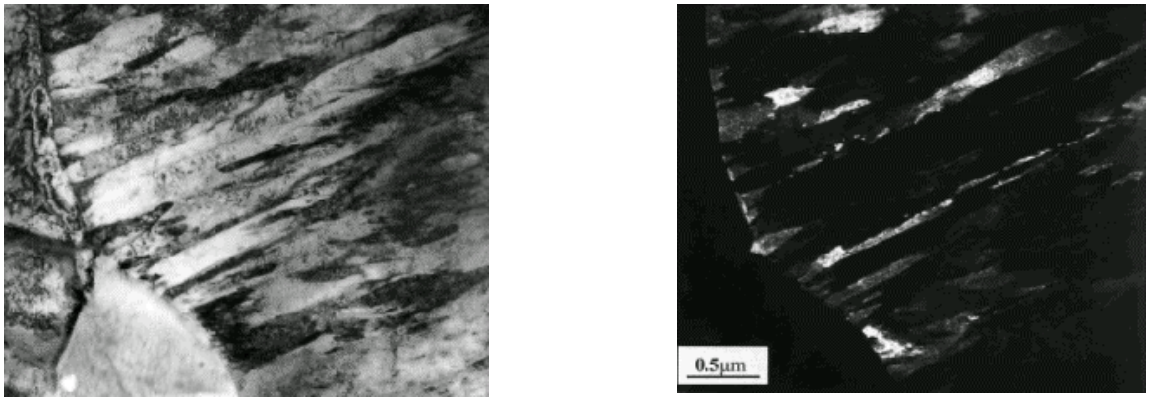

(a) (b)

Fig. 14 TEM micrographs of the Q&P microstructure produced by intercritical annealing (α_{IC}=25%) a 0.19%C-1.59%Mn-1.63%Si TRIP steel composition, followed by quenching to 260°C and partitioning at 400°C for 100 s: (a) bright-field image and (b) dark-field image using a (200) austenite reflection [9].

THE MECHANICAL PROPERTIES OF Q&P STEELS

Preliminary studies of mechanical properties generated in steels by the Q&P treatment have indicated differences from conventional heat treatments and the opportunity for potential improvements. For example, Fig. 15 illustrates how the relationship of elongation versus ultimate tensile strength for steels subjected to the Q&P process compares favorably with dual-phase, conventional TRIP and martensitic steels [7]. It also shows how Q&P could fill a gap in this ductility/strength continuum: compared with dual phase and conventional TRIP steels Q&P can offer increased strength, whilst compared with martensitic steels, it can offer increased ductility.

More recently, instantaneous n values (strain hardening) for a 0.19%C-1.59%Mn-1.63%Si composition subjected to a Q&P treatment after intercritical annealing at 820°C to produce 25% intercritical ferrite have been calculated from the expression [46]:

$$n_i = \left(\frac{\varepsilon p}{\sigma} \frac{d\sigma}{d\varepsilon} \right)$$

where n_i is an incremental work hardening parameter and ε_p is true plastic strain. Figure 16 compares instantaneous n values versus true plastic strain for two treatments: one curve, exhibiting negative slope, is for a sample quenched after intercritical annealing to produce 25% ferrite, showing behaviour typical of dual-phase steel [47], whilst the second curve, showing positive slope, is for a Q&P heat-treated sample. This sample was intercritically annealed to produce 25% intercritical ferrite, then quenched to 240°C and partitioned at 400°C for 30 s. A positive slope of instantaneous n versus plastic strain is suggestive of TRIP behavior [47].

HOME

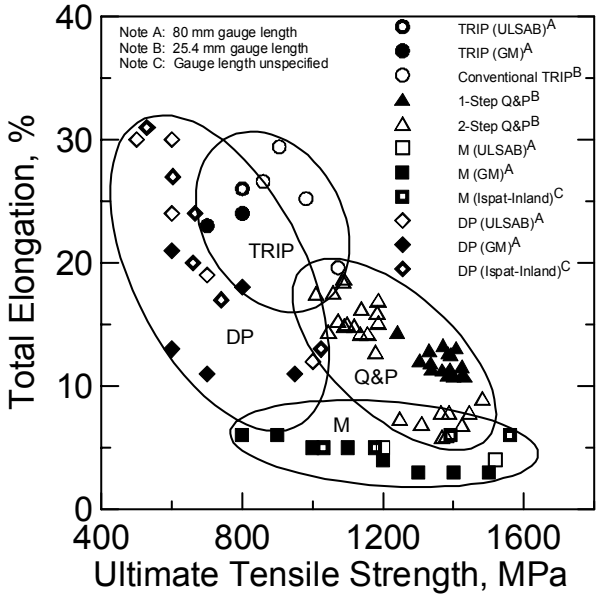

Fig. 15 Total elongation versus ultimate tensile strength for TRIP, dual phase (DP), martensitic (M), and Q&P sheet steel products [7].

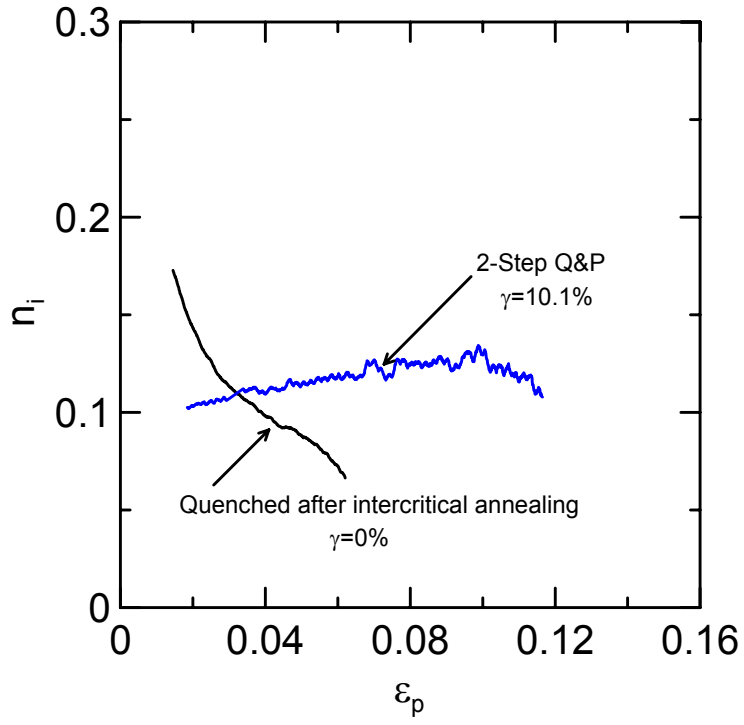

Fig. 16 Instantaneous n values versus plastic strain for a 0.19%C-1.59%Mn-1.63%Si steel composition, after intercritical annealing (dual-phase), followed by water-quenching, or after a Q&P heat-treatment. (Intercritical ferrite, α_{IC}=25%, for both conditions.)

HOME

SUMMARY

The thermodynamic background to the concept of a new heat treatment route, applicable to a range of steels, is described. The treatment involves quenching partially to martensite, followed by an anneal to allow carbon to partition from the martensite phase to the untransformed austenite, stabilising it against decomposition upon cooling back to room temperature. The new process has been called *quenching and partitioning* (*Q&P*) to distinguish it from quenching and tempering. The carbon is protected against carbide formation by suitable alloying. The kinetics of partitioning are shown to be important, not just to escape of the carbon from the martensite before carbide precipitation might occur, but possibly also to the extent of the final fraction of stable austenite through the progressive effective stabilisation across austenite regions before the final quench to room temperature. Emphasis is given to the likely evolution of the microstructure during the Q&P treatment, although for the steels of interest the first quench to produce the starting microstructure before the partitioning treatment is above room temperature where it is not straightforward to examine the microstructure directly. Alternative reactions to full partitioning are also given prominence, such as carbide precipitation and bainite formation. Finally, some preliminary mechanical property measurements are compared with customary steel conditions, particularly for formable steels, including dual-phase, TRIP and martensitic grades.

ACKNOWLEDGEMENTS

This research programme is currently being conducted under an international collaboration supported in the authors' respective countries by NSF *Grant # 0303510* (USA), EPSRC *Grant ref: GR/S86501* (UK) and CNPq *Grant Institutional Process # 69.0053/03-7* (Brazil). Support of the sponsors of the Advanced Steel Processing and Products Group at CSM are also acknowledged. POSCO, Ispat-Inland Steel Company, MACSTEEL, and North Star Steel, are acknowledged for providing experimental materials. The authors are also grateful to members of their respective research groups, in particular, Florian Gerdemann (RWTH-Aachen) and for discussions with colleagues.

REFERENCES

1) Fundamentals of Aging and Tempering in Bainitic and Martensitic Steel Products, Eds: G. KRAUSS and P.E. REPAS, ISS-AIME, Warrendale, PA, USA (1992).
2) J.G. SPEER, D.K. MATLOCK, B.C. DE COOMAN and J.G. SCHROTH, Acta Mater., 51, (2003), pp. 2611-2622.
3) J.G. SPEER, A.M. STREICHER, D.K. MATLOCK, F.C. RIZZO and G. KRAUSS, Austenite Formation and Decomposition, Eds: E.B. DAMM and M. MERWIN, TMS/ISS, Warrendale, PA, USA (2003), pp. 505-522.
4) D.K. MATLOCK, V.E. BRAUTIGAM and J.G. SPEER, Proc. THERMEC 2003, Trans Tech Publications, Uetikon-Zurich, Switzerland (2003), pp. 1089-1094.
5) J.G. SPEER, F.C. RIZZO, D.K. MATLOCK and D.V. EDMONDS, Proc. 59th Annual Congress of ABM, Sao Paulo, Brazil (2004), pp. 4824-4836.
6) J.G. SPEER, D.V. EDMONDS, F.C. RIZZO and D.K. MATLOCK, Current Opinion in Solid-State and Materials Science, 8, (2004), pp. 219-237.
7) A.M. STREICHER, J.G. SPEER, D.K. MATLOCK and B.C. DE COOMAN, Advanced High-Strength Sheet Steels for Automotive Applications, International Conference Proceedings, Ed: J.G. SPEER, AIST, Warrendale, PA, USA (2004), pp. 51-62.

HOME

8) F.C. RIZZO, D.V. EDMONDS, K. HE, J. SPEER and D.K. MATLOCK, Solid-Solid Phase Transformations in Inorganic Materials, PTM 2005, Phoenix, Arizona, Ed: J. HOWE, TMS, Warrendale, PA, 2005.
9) A. CLARKE, J.G. SPEER, D.K. MATLOCK, F.C. RIZZO, D.V. EDMONDS and K. HE, Solid-Solid Phase Transformations in Inorganic Materials, PTM 2005, Phoenix, Arizona, Ed: J. HOWE, TMS, Warrendale, PA, USA (2005).
10) D. V. EDMONDS, K. HE, F. C. RIZZO, B. C. DE COOMAN, D. K. MATLOCK and J. G. SPEER, International Conference on Martensitic Transformations, ICOMAT'05, Shanghai, China (2005).
11) R.F. HEHEMANN, Phase Transformations, ASM,, Metals Park, OH, USA (1970), pp. 397-432.
12) H.K.D.H. BHADESHIA and D.V. EDMONDS, Metall.Trans., 10A, (1979), pp. 895-907.
13) H.K.D.H. BHADESHIA, Bainite in Steels, Inst. Materials, Minerals and Mining, London, UK (1992).
14) H.K.D.H. BHADESHIA and D.V. EDMONDS, Metal Sci. J., 17, (1983), pp. 411-419.
15) H.K.D.H. BHADESHIA and D.V. EDMONDS, Metal Sci. J., 17, (1983), pp. 420-425.
16) V.T.T. MIIHKINEN and D.V. EDMONDS, Mater. Sci. Technol., 3, (1987), pp. 422-431.
17) V.T.T. MIIHKINEN and D.V. EDMONDS, Mater. Sci. Technol., 3, (1987), pp. 432-440.
18) V.T.T. MIIHKINEN and D.V. EDMONDS, Mater. Sci. Technol., 3, (1987), pp. 441-449.
19) F.G. CABALLERO, H.K.D.H. BHADESHIA, K.J.A. MAWELLA, D.G. JONES, and P. BROWN, Mater. Sci. Technol., 17, (2001), pp. 512-522.
20) C. GARCIA-MATEO, F.G. CABALLERO and H.K.D.H. BHADESHIA, ISIJ International, 43, (2003), pp. 1238-1243.
21) TRIP-Aided High Strength Ferrous Alloys, International Conference Proceedings, Ed: B.C. DE COOMAN, Technologisch Instituut VZW, Belgium (2002).
22) Advanced High-Strength Sheet Steels for Automotive Applications, International Conference Proceedings, Ed: J.G. SPEER, AIST, Warrendale, PA, USA (2004).
23) W.J. DUBENSKY and K.B. RUNDMAN, AFS Trans., 64, (1985), pp. 389-394.
24) V. FRANETOVIC, M.M. SHEA and E.F. RYNTZ, Mater. Sci. Eng., 96, (1987), pp. 231-245.
25) N. DARWISH and R. ELLIOTT, Mater. Sci. Technol., 9, (1993), pp. 572-602.
26) L. SIDJANIN, R.E. SMALLMAN and S.M. BOUTORABI, Mater. Sci., 10, (1994), pp. 711-720.
27) J. ARANZABEL, I. GUTIERREZ and J.J. URCOLA, Mater. Sci. Technol., 10, (1994), pp. 728-737.
28) A. HONARBAKHSH-RAOUF and D.V. EDMONDS, Electron Microscopy, ICEM 14, vol. II: Mater. Sci., (1998), pp. 173-174.
29) A. HULTGREN, Trans ASM (1947), p. 915.
30) M. HILLERT, Jernkont. Ann., 136, (1952), p. 25.
31) E. RUDBERG, Jernkont. Ann., 136, (1952), p. 91.
32) M. HILLERT and J. AGREN, Scripta Mater., 50, (2004), pp. 697-699.
33) J.G. SPEER, D.K. MATLOCK, B.C. DE COOMAN and J.G. SCHROTH, Scripta Mater., 52, (2005), pp. 83-85.
34) M. HILLERT and J. AGREN, Scripta Mater., 52, (2005), pp. 87-88.
35) G. KRAUSS, Steels: Heat Treatment and Processing Principles, ASM International, Metals Park, OH, USA, (1990).
36) F.L.H. GERDEMANN, Microstructure and Hardness of 9260 Steel Heat-Treated by the Quenching and Partitioning Process, Diploma Thesis, Aachen University of Technology, Germany, (2004).
37) H.K.D.H. BHADESHIA, Acta Metall., 28, (1980), pp. 1103-1114.
38) A. BORGENSTAM, A. ENGSTRON, L. HOGLUND and J. AGREN, J. Phase Equilibria, 21, (2000), pp. 269-280.
39) M. HILLERT, L. HOGLUND and J. AGREN, Acta Metall. Mater., 41, (1993), pp. 1951-1957.

HOME

40) W.S. OWEN, Trans ASM, 46, (1954), pp. 812-829.
41) J. GORDINE and I. CODD, J. Iron Steel Inst., 207, (1969), pp. 461-467.
42) W. C. LESLIE and G.C. RAUCH, Metall. Trans., 9A, (1978), pp. 343-349.
43) S.J. MATAS and R.F. HEHEMANN, Trans Met. Soc. AIME, 221, (1961), pp. 179-185.
44) B.P.J. SANDVIK, Metall. Trans., A13, (1982), pp. 777-787.
45) S.J. BARNARD, G.D.W. SMITH, A.J. GARRATT-REED and J. VANDER SANDE, Advances in the Physical Metallurgy and Applications of Steels, Metals Soc., London, UK, (1981), pp. 33-38.
46) D.K. MATLOCK, F. ZIA-EBRAHIMI and G. KRAUSS, Deformation, Processing and Structure, Ed: G. KRAUSS, (1984), American Society for Metals, Metals Park, OH, pp. 47-87.
47) O. YAKUBOVSKY, N. FONSTEIN and D. BHATTACHARYA, TRIP-Aided High Strength Ferrous Alloys, International Conference Proceedings, (2002), pp. 263-270.

HOME